JOURNAL OF MATERIALS SCIENCE 33 (1998) 3899–3906

Laser ultrasonic monitoring of aluminium alloy microstructural evolution

J. B. SPICER, S. L. WALLACE*
The Johns Hopkins University, Department of Materials Science and Engineering, Baltimore, MD 21218, USA
E-mail: spicer@jhurms.hcf.jhu.edu

The laser ultrasonic monitoring of aluminium alloy microstructural development during thermal processing is demonstrated. This monitoring is based on the ability to measure the differential ultrasonic attenuation in alloy systems. Differential attenuation is related to anelastic physical processes which are active during microstructural evolution. For the aluminium alloys studied, these anelastic effects derive from alloying species solution and mobility. Methods have been outlined for separating processes which affect the physical properties but are not related to microstructural changes from those properties which are linked to microstructural evolution. © *1998 Kluwer Academic Publishers*

1. Introduction

Ultrasonic property variations in metals and metal alloys have been studied extensively and have been used to infer the microstructural states of these materials. The modulus variations which accompany temperature changes have been quantified for numerous alloy systems [1] and have been used to estimate the internal temperatures in alloy ingots which are being thermally treated [2]. Previous work using laser-induced ultrasound in various alloy systems has quantified ultrasonic velocities as a function of temperature; in particular, measurements through the liquidus and solidus temperatures in aluminium alloys have been presented, showing effects of alloying constituents [3]. Unfortunately, a functional relationship between the state of the material and the ultrasonic properties does not occur in general since multiple aspects of the state affect the ultrasonic properties. For example, variations in crystalline grain orientation in alloys can affect ultrasonic velocities [4] as much as externally applied temperature variations do. In addition, microstructural variation as a result of thermal treatment may occur, producing coupled influences on the ultrasonic properties. Sufficiently precise ultrasonic measurements of longitudinal velocity have been used to elucidate and separate various influences on the ultrasonic properties of aluminum alloys undergoing heat treatment [5]. The precision required for these measurements of ultrasonic wave speed approached 0.03% and was achieved using momentary contact methods on the samples at elevated temperatures. Generally, ultrasonic attenuations are affected by microstructural variations more strongly than are the corresponding ultrasonic velocities and may be used to assess microstructural states; however, the precision of attenuation measurements is generally low compared with ultrasonic velocity measurements owing to the difficulties involved in making attenuation measurements especially at elevated temperatures [6, 7].

Continuous monitoring of ultrasonic properties at elevated temperatures may be performed using laser ultrasonic methods [8]. Owing to the remote nature of these sensor methods, ultrasonic data may be acquired without incurring significant effects on the overall temperature or microstructure of the material. Laser ultrasonic monitoring of ultrasonic velocities in various materials systems undergoing thermal treatment has been conducted by various groups [9–11]. The results of these studies indicate that the precision of ultrasonic velocity measurements using laser-based methods is about 0.1% which is not quite sufficient to separate subtle microstructural effects on velocity from larger temperature-driven effects. To achieve the stated precision for velocity determination, the results in these studies were obtained predominately using an ablative laser source. The ablative source removes material from the sample surface at sufficiently high laser pulse fluences and produces large forward-directed longitudinal waves which improve the signal-to-noise of the corresponding ultrasonic signals. The increased signal-to-noise ratio for these signals allows relatively precise determination of times of flight when compared with non-ablative laser generation of ultrasound. In addition, it is noted that the highest frequencies in the laser ultrasonic signal are quite sensitive to the microstructure of the material, and it has been shown that for ablative laser sources, the signal-to-noise ratio for high frequencies is sufficient to determine aspects of aluminium alloy microstructure [12].

* *Present address*: Massachusetts Institute of Technology, Department of Materials Science and Engineering, Cambridge, MA, 02139, USA.

However, the signal-to-noise ratio at these frequencies for thermoelastic generation is small. Unfortunately, the sample surface is changed by the ablation process, introducing a source of uncertainty into the measurement. Additionally, other information in the laser ultrasonic signal is not enhanced by the ablation process; the longitudinal wave amplitude increases, but the shear wave signal amplitude does not. In general, the laser source produces both longitudinal and shear waves which propagate from the source to the ultrasonic receiver interacting with essentially the same volume of material. Ultrasonic interrogation using longitudinal and shear waves may be conducted nearly simultaneously using laser ultrasonic methods. Consequently, compared with conventional contacting techniques, laser methods may be used to provide significantly more ultrasonic information about a given state of the material microstructure. However, the ablative laser source does not improve the forward-directed shear wave signal and, as such, does not exploit the full character of the laser source.

At laser pulse fluences below the onset of ablative processes, laser ultrasonic wave generation occurs by the thermoelastic effect where the laser pulse energy is absorbed by the material, rapidly heats and expands the irradiated region launching ultrasonic waves into the material. The thermoelastic laser ultrasonic source is well understood and has been studied by many workers [13]. However, even though the thermoelastic laser source has unique characteristics as an ultrasonic source, these characteristics have not been fully exploited in the determination of materials microstructural evolution during thermal processing. In this paper, thermoelastic laser source theory is examined to identify aspects of the theory which aid the ultrasonic monitoring of materials microstructure. These aspects are combined with ultrasonic wave scattering theory to develop simple expressions for experimental data analysis. Laser ultrasonic results obtained during thermal treatment of various aluminium alloys are analysed using these expressions and are used to identify aspects of microstructural evolution in these alloys. In particular, the dissolution of secondary phases is identified indicating the potential of the method for real-time *in-situ* determination of solution temperatures in systems which exhibit precipitation-hardening effects.

2. Theory

The seminal principle to the current work is to identify those laser ultrasonic source characteristics which may be exploited to monitor microstructural changes in aluminium alloys continuously during thermal processing. As a guide to the results presented, the overall issues concerning laser ultrasonic monitoring of aluminium alloy microstructure will be outlined. The essential theory surrounding these issues will be given in detail sufficient to justify the analysis of experimental results. Previous work on aluminium alloys has shown that the effects of microstructural changes on longitudinal wave velocity are small [5]. Unfortunately, the signal-to-noise characteristics of thermoelastic laser ultrasonic signals generally do not approach those required for precise wave speed determination for microstructural monitoring. The associated changes in ultrasonic attenuation have been shown to be relatively large in other alloy systems and should provide valuable information regarding the alloy microstructural state [6]. Conveniently, laser ultrasonic methods for attenuation measurements have been investigated previously where conventional ultrasonic methods for attenuation determination were applied to laser-induced ultrasound. An ablative laser source was required to produce forward-directed ultrasound of sufficient amplitude to apply conventional attenuation measurement methods to laser ultrasonic signals and, consequently, only longitudinal wave interactions with the microstructure were quantified [14]. However, it is well known that ultrasonic shear waves interact with a given material microstructure differently from the way in which longitudinal waves do. In particular, in polycrystalline materials, the longitudinal and shear wave attenuations differ and depend intimately on a range of materials properties including grain size and elastic moduli [15]. A simultaneous measurement of the longitudinal and the shear wave attenuations may be used to identify microstructural variations in alloys undergoing thermal processing.

Since the thermoelastic laser source generates both longitudinal and shear waves, it would appear that this type of ultrasonic source may be used to measure both attenuations in an alloy. Unfortunately, the ultrasonic wave amplitudes from the thermoelastic laser source preclude accurate determination of attenuation using conventional analysis techniques. In particular, if the epicentral laser ultrasonic waveform is considered (Fig. 1), the signal amplitudes for the dominant features vary as l^{-2} where l is the source-to-receiver separation or the plate thickness. Consequently, signal amplitudes rapidly decrease as the ultrasound traverses a plate structure. Additionally, changes to the microstructure which impose signal attenuations beyond those expected from the noted

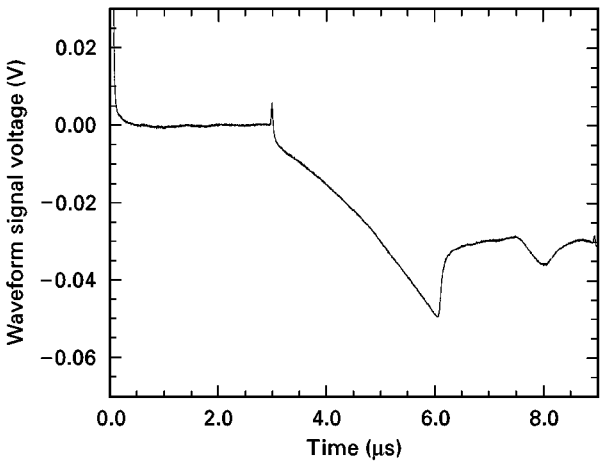

Figure 1 Experimental epicentral laser ultrasonic waveform obtained in aluminium alloy 1100. The step-like discontinuities in the waveform which occur at approximately 3 and 6 μs correspond to the arrival of longitudinal and shear waves, respectively.

geometrical effects may preclude independent assessment of the wave attenuations. However, if absolute determination of attenuation is not required and only accurate indication of microstructural variation is needed, then the relative attenuation between the longitudinal and shear waves may be sufficient to characterize material evolution. For wave propagation through a fixed amount of material, the relative attenuation may be inferred by direct comparison of the step displacements which occur at the ultrasonic arrival times.

Simple detection of the displacement amplitudes would be sufficient if the thermal and optical properties and the elastic stiffnesses were constant; however, as the material temperature changes, all these properties vary as a result of intrinsic material behaviour or as a result of changing surface conditions. The effects of these property variatons must be minimized to extract information which is linked intimately to the microstructure. The relative attenuation measurement minimizes the effects of thermal and optical property changes since the longitudinal and shear displacements have the same functional dependence on these properties. Unfortunately, intrinsic temperature-induced modulus variations affect the displacement amplitudes such that their ratio and, consequently, the relative attenuation would apparently change with temperature. These modulus-driven effects may be eliminated if results for the description of laser ultrasound are used [16]. Similarly, another source for differential attenuation which is not linked to microstructural variations is grain scattering in crystalline materials. Grain scattering is strongly influenced by the material moduli such that modulus changes not linked to microstructural variations would affect the differential attenuation. Fortunately, these variations may be taken into account using the results of ultrasonic scattering theory [15]. Given the ability to compensate for modulus changes, a meaningful indicator of microstructural variations is the relative displacement amplitudes accompanying the longitudinal and shear waves in the epicentral laser ultrasonic waveform.

To derive quantitative relationships for data analysis, the essential aspects for the theory of thermoelastic laser ultrasonic wave generation in metal alloys is reviewed. This theory has been studied extensively and has been the subject of numerous investigations which have concentrated on divers aspects of the laser ultrasonic process [16–21]. For a material containing varied microstructural elements, the analysis of the laser ultrasonic process is quite involved; however, if the material may be represented by an isotropic homogeneous solid, then the required results may be derived directly. For the development presented here, it is assumed that effects of microstructure may be imposed on the results obtained for the isotropic homogeneous solid.

Consider the experimental geometry shown in Fig. 2a where a laser pulse impinges on one surface of a plate and the resulting ultrasonic displacements are measured on the opposite side of the plate. The receiver position is directly opposite that of the source in

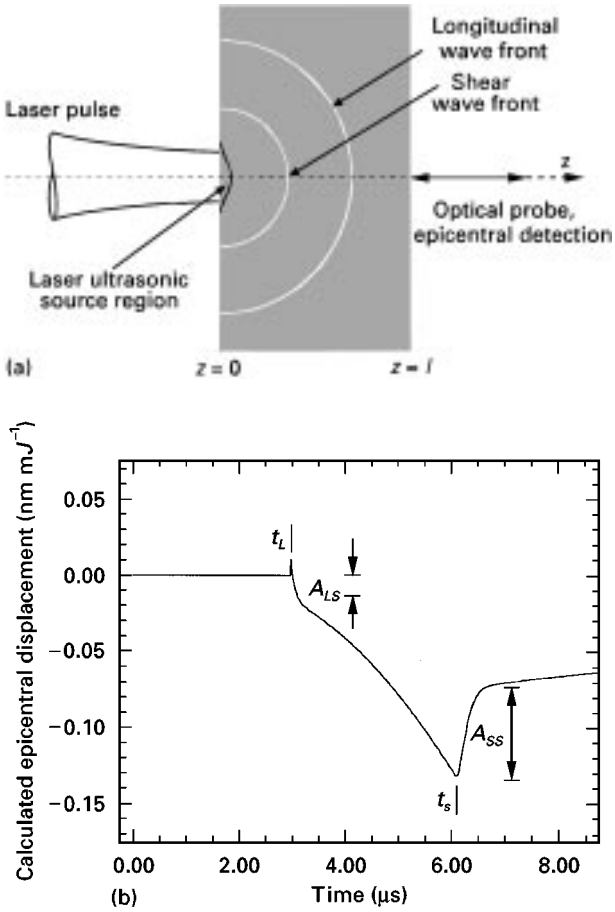

Figure 2 (a) Detection geometry for the epicentral waveform produced by a laser source. (b) Calculated epicentral waveform showing the times of arrival and the amplitudes of the ultrasonic modes used in this study.

the epicentre location. If the plate is sufficiently thick that thermal disturbances generated at the source do not interact with the material at the receiver location during the times of interest, then the plate appears to be thermally thick. Given these conditions, it has been shown that the laser source may be modelled using an equivalent elastic source acting at the surface of the plate [19]. As this source approaches the limiting characteristics of a spatially point-like temporal impulse in a material of vanishing thermal conduction, the displacements occurring at the epicentre receiver may be derived analytically [16]. The displacement versus time waveform for early times using a spatially and temporally finite source is shown in Fig. 2b. For the times of this waveform, the features of interest are the step-like displacements which occur at the longitudinal and the shear wave arrival times, t_L and t_S, respectively. Since these displacements result from a common-thermal-expansion source, the amplitudes of these displacements are related by the elastic moduli of the material. Indeed, for a point impulse source in a thermally non-conductive material, the following result has been derived relating the displacements and the elastic constants in the material [16]:

$$\frac{A_{SS}}{A_{LS}} = -\frac{2(1-\nu)}{1-2\nu} \tag{1}$$

where A_{SS} is the amplitude of the step which occurs at the shear time of arrival (shear step), A_{LS} is the step amplitude at the longitudinal time of arrival (longitudinal step) and ν is the Poisson ratio for the material. This elegant analytical result may be adapted for use in examining experimental observations by converting the Poisson ratio to elastic moduli (the Lamé constants) and then to elastic wave speeds. The result is given as follows:

$$\left|\frac{A_{SS}}{A_{LS}}\right| = \frac{c_1^2}{c_2^2} \tag{2}$$

where c_1^2 is the longitudinal wave speed, c_2^2 is the shear wave speed and the absolute value sign merely yields the magnitude of the ratio without the relative displacement directions. Typically, wave speeds are calculated on the basis of a wave time of flight and a dimensional measurement; however, since the wave speeds appear in ratio to one another, the sample dimension does not enter into the expression for the displacement ratio. That the relationship is sample dimension independent is quite useful in that it eliminates the need to perform measurements outside the laser ultrasonic measurement. Using expressions for the wave speeds, the amplitude ratio is expressed in terms of the wave times of flight as follows:

$$\left|\frac{A_{SS}}{A_{LS}}\right| = \frac{t_S^2}{t_L^2} \tag{3}$$

where t_S is the time of flight for the shear step and t_L is the time of flight for the longitudinal step. Not only does this equation hold regardless of sample dimension, but also it is independent of the thermal and the optical properties of the material so long as the previous assumptions concerning the source continue to obtain. The results of more accurate laser source modelling, which are shown in Fig. 2, indicate that the effects of finite source size and laser pulse duration do not significantly alter the relationship given in Equation 3 for the current work. Consequently, as an aluminium alloy is thermally processed, laser ultrasonic data can be analysed to provide information concerning the expected variation in the ultrasonic mode amplitudes regardless of changes in surface reflectivity, material thermal properties, sample length or elastic moduli. The result given in Equation 3 should hold unless microstructural effects cause the material to behave differently from an isotropic continuum.

One effect which produces experimental deviations from the predicted behaviour in Equation 3 is grain scattering in materials. The effects of grain scattering on the relative attenuation between the longitudinal and shear waves may be expressed conveniently if the following conditions hold:

(i) The grain size in the material is small compared with the ultrasonic wavelength.
(ii) Variations in moduli from grain to grain are small.
(iii) Grains are randomly oriented such that the bulk material behaves isotropically.

Using these assumptions, the results for the relative amplitudes of the steps in the epicentral laser ultrasonic waveform could be modified; however, the length of the derivation prevents its investigation in this work. Rather, previous results for the ratio of the attenuation coefficients will be repeated as follows:

$$\frac{\sigma_S}{\sigma_L} = \frac{3}{4}\frac{c_1^3}{c_2^3} = \frac{3}{4}\frac{t_S^3}{t_L^3} \tag{4}$$

where σ_S is the attenuation coefficient for the shear wave and σ_L is the longitudinal wave attenuation coefficient [15]. In Equation 4, substitutions for the wave speeds in terms of experimentally measurable times of flight have been made. As was found for the amplitude ratio from laser ultrasonic theory, this ratio is independent of sample length.

The results given in Equations 3 and 4 may be combined to yield a new relationship between the times of flight and the amplitudes which includes the effects of grain scattering. This expression is given as follows:

$$\ln\left|\frac{t_S^2}{t_L^2}\frac{A_{SS}}{A_{LS}}\bigg|_{z=l}\right| = (\sigma_L\, l)\left(\frac{3}{4}\frac{t_S^3}{t_L^3} - 1\right) \tag{5}$$

where l is the ultrasonic propagation length which is nominally the sample thickness. Equation 5 is of the form $y = (m)x$ with the slope yielding the attenuation coefficient for the longitudinal wave if the sample length is known. The grouping of measurables $y = \ln|t_S^2/t_L^2/A_{LS}/A_{SS}|_{z=l}|$ will be referred to as the laser ultrasonic group, and $x = 3/4t_L^3/t_S^3 - 1$ as the attenuation group. In the absence of attenuation resulting from grain scattering, the laser ultrasonic amplitude ratio holds and both sides Equation 5 are equal to zero. Amplitude effects which are related to modulus changes at the source and through the bulk of the material are described by Equation 5. However, if an attenuation mechanism other than grain scattering manifests itself during thermal treatment, then the description provided by Equation 5 fails to hold and the linear relationship between the laser ultrasonic group and attenuation group is not expected.

Grain scattering in aluminium alloys is generally small and, consequently, the laser ultrasonic group should be approximately zero. However, as the temperature of an aluminium alloy is raised, anelastic processes contribute to the ultrasonic attenuation. These processes can be linked primarily to the mobility of solutionized alloying elements in the microstructure at temperatures above the solvus. This mobility is generally linked to vacancies in the microstructure which aid the diffusion of alloying species. However, in general, a range of physical processes affect the anelastic response of aluminium alloys at ultrasonic frequencies and the description of the functional dependence of attenuation on these processes is incomplete. Regardless, if it is assumed that the longitudinal wave attenuation in the alloy is linked to the mobility of alloying species, then a form for the attenuation may be arrived at as follows:

$$\sigma_L = \sigma_{0L}\left[1 + \alpha\exp\left(-E\sqrt{k_B T}\right)\right] \tag{6}$$

where σ_{0L} is an attenuation coefficient which is related solely to scattering processes, α is an amplitude factor

for anelastic grain scattering, E is the activation energy for the anelastic attenuation process, k_B is the Boltzmann constant and T is the absolute temperature. At low temperatures, the grain scattering attenuation should not be affected by anelastic processes; however, as the temperature increases, anelastic processes should contribute to the attenuation. Owing to the uncertainty concerning the actual processes which actively contribute to the attenuation in various aluminium alloys, a single effective activation energy will be assumed and will be used in the experimental data analysis.

Both the laser ultrasonic group and the attenuation group are composed of experimentally measurable quantities. Consequently, if the ultrasonic propagation length is known approximately, then the attenuation may be determined and may be measured as a function of temperature. According to Equation 6, attenuation variation does not reflect abrupt, changes in microstructure but is continuous with temperature in aluminium alloys and is linked to diffusing species number and mobility. Experimental results may be analysed using Equations 5 and 6 to demonstrate laser ultrasonic monitoring of aluminium alloy microstructural evolution. In particular Equations 5 and 6 are combined as follows:

$$\ln\left[\ln\left|\frac{t_S^2}{t_L^2}\frac{A_{LS}}{A_{SS}}\right|_{z=l}\Bigg/\left(\frac{3}{4}\frac{t_S^3}{t_L^3}-1\right)-\sigma_{0L}l\right] = \ln(\alpha\sigma_{0L}l)+\left(-E\sqrt{k_BT}\right) \quad (7)$$

which represents the laser ultrasonic data as a function of temperature and indicates that the subtraction of a constant, $\sigma_{0L}l$, from the experimental data will allow an activation energy to be determined from the data. Unfortunately, at the frequencies of interest, the low-temperature grain scattering in aluminium alloys is small and the laser ultrasonic group is close to zero. Owing to signal-to-noise considerations, the ratio of the laser ultrasonic group to the attenuation group varies about the constant, $\sigma_{0L}l$, such that, when this constant is subtracted from the data according to Equation 7, the logarithm argument may be negative for low-temperature data. For the results in the current work, only high-temperature data for which the ultrasonic signal-to-noise ratio is sufficient to apply Equation 7 may be used to extract information about the activation energy of the anelastic attenuation process.

3. Experiment

The materials chosen for study in this work included aluminium alloys 2024, 7075 and 1100. Aluminium alloys 2024 and 7075 were chosen on the basis of their well-understood metallurgical behaviour during thermal treatment. These materials contain a range of alloying constituents which are solutionized at elevated temperatures and precipitate under equilibrium conditions to form secondary phases at low temperatures [22]. Aluminium alloy 1100 was chosen as a reference material; it is commercially pure aluminium with only residual tramp impurities which do not form phases with solvus temperatures in the range investigated in this work. Multiple samples of each alloy were prepared as discs, approximately 19 mm thick and 50 mm in diameter, with one face on each disc polished to a mirror surface and the other face not being specially prepared beyond the original lathe finish. All samples were subjected to a high temperature thermal treatment to remove any residual stresses and to normalize the microstructure. The samples were furnace cooled to produce the equilibrium microstructures of the various alloys.

The experimental apparatus used for the laser ultrasonic monitoring of the aluminium alloys as a function of temperature is shown schematically in Fig. 3. An alloy sample was placed near one end of a box furnace where optical access to the sample was provided by clearance holes in the front and back insulation materials. The atmosphere in the furnace was not controlled and was open to the laboratory environment. Heating of the furnace was controlled by manual adjustment of the temperature set point of the furnace controller unit. The temperature was monitored and adjusted using the furnace thermocouple. All ultrasonic data were recorded at various fixed and equilibrated temperatures for the furnace thermocouple. The sample temperature was inferred through calibration of the furnace thermocouple to a second thermocouple placed at the sample position in the furnace.

A Molectron MY 32, pulsed neodymium-doped yttrium aluminium garnet laser (pulse full width at half-maximum, about 16 ns; pulse energy, about 60 mJ) was used for generation of ultrasound. The laser pulse fluence was adjusted using a focusing lens to yield a spatially restricted source while maintaining ultrasonic generation in the thermoelastic regime. The ultrasonic transients were detected using a modified Michelson-type stabilized interferometer. This type of interferometer is sensitive to surface displacements and is inherently uniform in its frequency response characteristics [23, 24]. The interferometer signal was recorded using a digital oscilloscope at a sampling

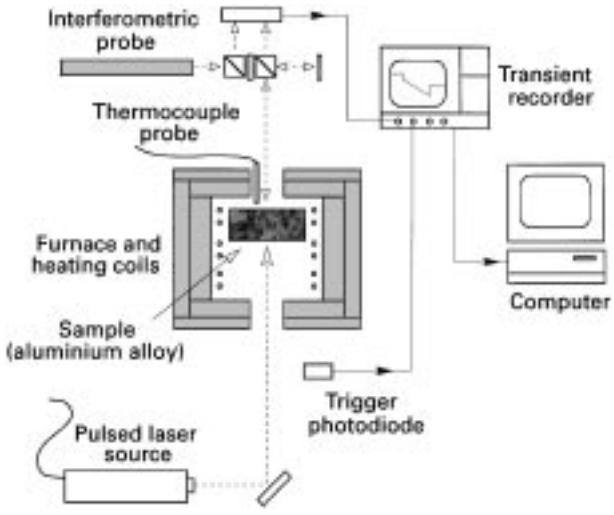

Figure 3 Schematic diagram of the experimental apparatus for laser ultrasonic monitoring of aluminium alloys subjected to thermal processing.

rate of 500 M samples s^{-1} and was transferred to a computer for data storage and analysis. For the experimental results presented in this work, the interferometer bandwidth was limited to about 60 MHz and was sufficient for recording the necessary displacement data for analysis. Ultrasonic detection was performed on epicentre to the source; this position was determined through ultrasonic alignment of the source and receiver and was maintained throughout the experiment while the sample was heated.

Owing to the low power of the interferometer laser (about 8 mW), the sample surface had to be in mirror-like condition to provide adequate signal-to-noise ratio for the recorded transient signals. Laser noise in these signals required that ten waveforms be averaged to provide sufficient signal-to-noise ratio for data analysis. These waveforms were averaged over a 1–2 s signal acquisition time with the temperature being held constant during this time. At temperatures in excess of about 540 °C, surface oxidation decreased the sample reflectivity irreversibly during the time of the study. Consequently, ultrasonic data could not be gathered during sample cooling and were gathered solely during sample heating.

4. Results

Velocity calculations for the longitudinal and shear waves were made for all waveforms as a function of temperature. The sample dimension was taken to be the initial sample length; corrections for thermal expansion were not made since this correction is negligibly small for the data shown. Times of flight for longitudinal waves were taken from the time origin to the beginning of the precursor [21]; those for the shear step were taken from the origin to the displacement minimum at the beginning of the shear step. Typical results for aluminium alloys 1100, 2024 and 7075 are shown in Fig. 4 where the longitudinal and shear wave speeds are shown as functions of temperature. The velocity variation with temperature for aluminium alloy 1100 is shown in both graphs to establish a baseline from which the effects of alloying constituents may be assessed qualitatively. Additionally, the aluminium alloy 7075 data represent the results obtained on two different samples to indicate the reproducibility of results from sample to sample. The curves shown with the points are provided to associate those points which belong to a given data set. For all samples, the decreases in wave speed with increasing temperature are indicative of intrinsic moduli reductions. The differences between the temperature dependence of the wave speed of pure aluminium and those of the other materials are attributable primarily to intrinsic moduli changes brought about by the alloying constituents. Additionally, anelastic processes contribute to wave speed variation at the higher temperatures where the points for the alloys deviate considerably from those for the pure aluminium [5]. The results presented here are not sufficiently precise to determine quantitatively the functional dependence of the wave speeds on these processes; however, the results are consistent with previous work on aluminium where

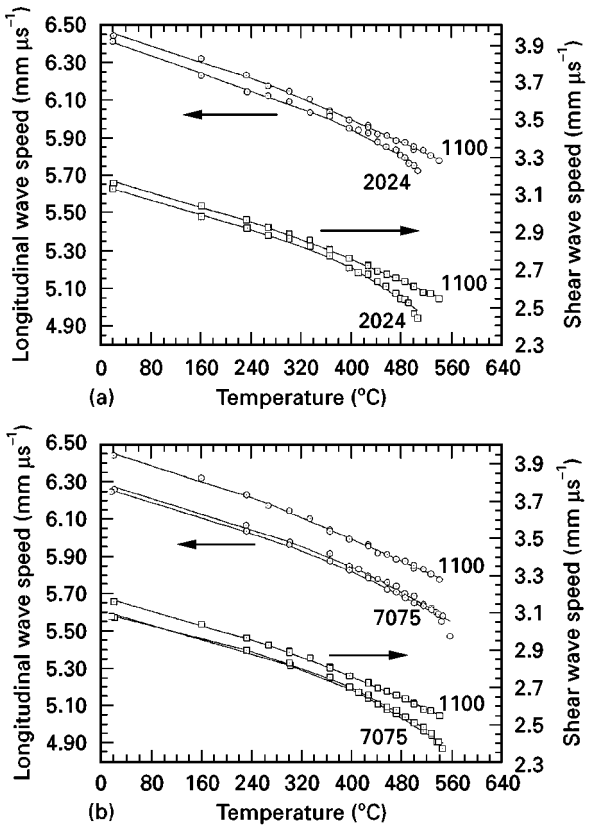

Figure 4 (a) Ultrasonic velocities for aluminium alloys 1100 and 2024 as functions of temperature. Ultrasonic data were obtained for aluminium alloy 1100 to higher temperatures than for aluminium alloy 2024 owing to the solidus temperature for aluminium alloy 2024 which is significantly lower than the nominal melting temperature for aluminium alloy 1100. (b) Ultrasonic velocities for aluminium alloys 1100 and 7075 as functions of temperature. The data from two samples of aluminium alloy 7075 have been used to construct this graph to demonstrate measurement consistency.

formulae were given for the temperature variation of longitudinal wave speeds in various alloy systems [5].

Ultrasonic amplitude variations are expected to accompany the modulus changes indicated by the ultrasonic velocity data. Measurements of the step amplitudes for the longitudinal and shear arrivals were made according to the prescription shown in Fig. 2. It is noted that the onsets of these arrivals are quite abrupt and the corresponding signal level is easily determined. The signal amplitude at the end of these steps is not so easily determined owing to the smoothly varying nature of the signal. Various methods have been employed to determine the step amplitudes from the experimental waveforms; all these methods yield results that are in general agreement with one another. The first method uses the extrema of the second temporal derivative of the signal to indicate step initiation and termination. A second uses linear fits to the data immediately after step onset and after step termination to produce an intercept that indicates step amplitude at termination. A third method that was robust and was most directly automated employed error minimization signal processing algorithms to fit theoretically derived waveforms using Rose's [16] theory to the experimental waveforms.

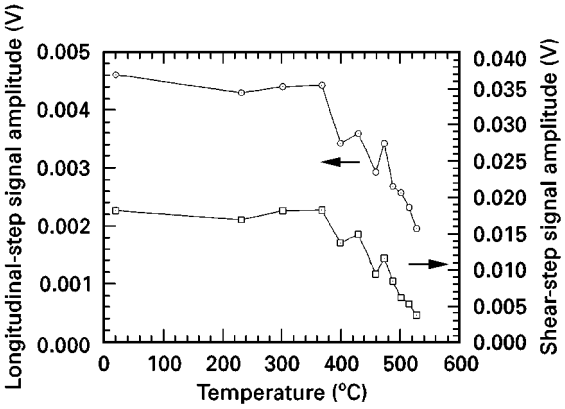

Figure 5 Ultrasonic signal amplitudes for the longitudinal and shear steps as functions of temperature. These signals depend on a range of factors and cannot be used as direct indicators of actual ultrasonic amplitudes.

The step amplitudes were extracted directly from the theoretical waveforms.

Ideally, the amplitude variations extracted using these methods should depend solely on the modulus; however, the relation between ultrasound amplitude and modulus does not follow directly from the laser ultrasonic waveforms. In Fig. 5 the signal amplitudes associated with the longitudinal and shear steps are shown as a function of temperature for one of the aluminium alloy 7075 samples. The signal amplitudes generally decrease as the temperature increases. As was discussed previously, the decrease in signal amplitude could result from changes in the thermal and optical properties, from changes in the material moduli or from increases in the ultrasonic attenuations. Variations in thermal and optical properties may be minimized by considering the ratio of the step amplitude signals. Remaining effects related to changes in the moduli may be taken into consideration using the laser ultrasonic group and the attenuation group according to Equation 5. Any remaining dependence of the signal on temperature must result from microstructural variations occurring in the material and may be described using the result derived in Equation 7.

Applying the analysis suggested by Equation 7 to the data obtained on the aluminium alloy 1100 sample produces the results shown in Fig. 6a where the ratio of the laser ultrasonic group to the attenuation group less a constant is shown as a function of the reciprocal temperature. The solid line represents the least-squares linear fit to the data. The data suggest that through the temperature range of investigation, no significant changes occur to the aluminium microstructure. At the maximum temperature, there may be effects related to dislocation interactions; however, the results presented here do not justify comment to these effects. By contrast, analysis results for the data from the aluminium alloy 7075 samples using Equation 7 are shown in Fig. 6b. Data sets from aluminium alloy 7075 samples are represented using different data point markers: open squares for sample A and open circles for sample B. The solid curve in this figure represents the least-squares fit to the data for sample

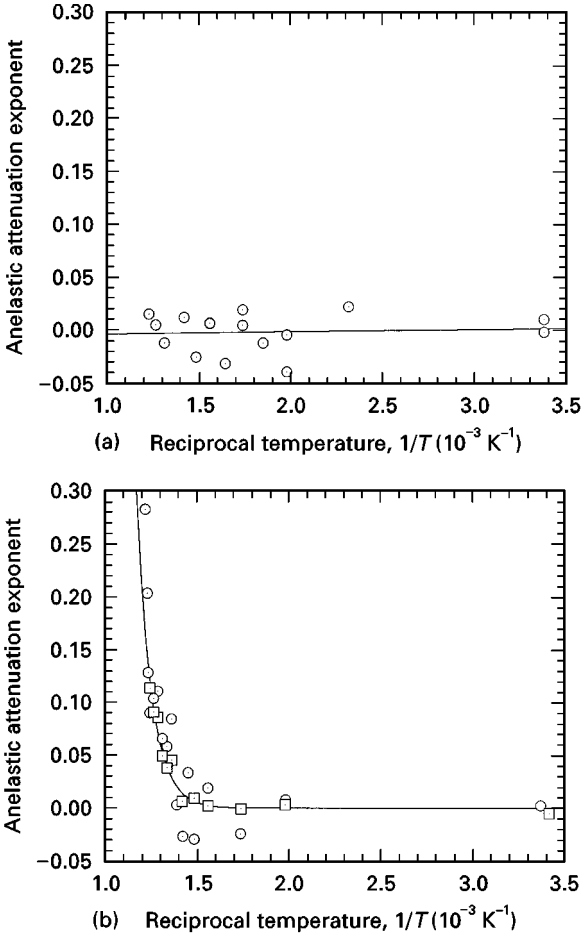

Figure 6 (a) Anelastic attenuation in aluminium alloy 1100 as a function of reciprocal temperature. These results indicate that thermally induced anelastic effects do not contribute to the ultrasonic attenuation in the temperature range studied. (b) Anelastic attenuation in aluminium alloy 7075 as a function of reciprocal temperature. The solid curve is an exponential function which represents the least-squares fit to the data for one of the aluminium alloy 7075 samples.

A using an exponential function where, owing to signal-to-noise considerations, only the high-temperature data points were used in deriving the curve. The effective activation energy associated with the curve shown is 1.06 eV which is consistent with activation energies for diffusion related phenomena in aluminium [25]. Clearly, the anelastic effects related to alloying species solution have been separated from processes which affect the physical properties but do not represent microstructural changes.

Similar results to those presented for aluminium alloy 7075 were obtained for aluminium alloy 2024. Unfortunately, the signal-to-noise characteristics for the aluminium alloy 2024 results were not adequate to extract a meaningful value for the effective activation energy even though reasonable results were obtained for the wave speed measurements. For all the waveforms recorded, the longitudinal step amplitude was less than that of the shear step, and the resulting accuracy of the step ratio, present in the laser ultrasonic group, is limited by the signal-to-noise ratio of the longitudinal step. At elevated temperatures, the step signals decrease owing to lowered surface reflectivity even as the anelastic effects become significant.

The resulting degradation of the longitudinal step signal introduced significant error into the analysis for several of the intermediate temperature data points for the aluminium alloy 2024 material. At intermediate temperatures the anelastic effects were small while signal levels were diminished. Improvements to the interferometer components would directly enhance the detection of the anelastic effects at the elevated temperatures.

5. Conclusions

The laser ultrasonic monitoring of aluminium alloy microstructural development during thermal processing has been demonstrated. This monitoring is based on the ability to measure the differential ultrasonic attenuation in alloy systems. This attenuation is related to anelastic physical processes which occur during microstructural evolution. For the aluminium alloys studied, these anelastic effects were related to alloying species solution. Methods have been outlined for separating processes which affect the physical properties but are not related to microstructural changes from those properties which are linked to microstructural evolution. These methods are conceptually simple and could be performed to identify microstructural changes in aluminium alloys *in situ* during thermal processing. For aluminium alloy 1100, the analysis of the laser ultrasonic data indicated that no significant microstructural changes occurred throughout the temperature range of this study. Results for aluminium alloy 7075 indicated that significant changes to the microstructure occurred and that these changes were brought about by thermally activated processes which had an effective activation energy of 1.06 eV. This value for the effective activation energy can be compared favourably with those for diffusional processes in aluminium.

Acknowledgement

This material is based upon work supported in part by the US Department of the Army, Army Research Laboratory under Cooperative Agrement DAAL01-96-2-0047.

References

1. Y. TAKEUTI, S. KOMORI, N. NODA and H. NYUKO, *J. Therm. Stresses* **2** (1979) 233.
2. H. N. G. WADLEY, S. J. NORTON, F. MAUER and B. DRONEY, *Phil. Trans. R. Soc.* **320** (1986) 341.
3. A. IDRIS, C. EDWARDS and S. B. PALMER, *Nondestr. Test. Eval.* **11** (1994) 195.
4. F. E. STANKE and G. S. KINO, *J. Acoust. Soc. Amer.* **75** (1984) 665.
5. W. JOHNSON, F. MAUER, D. PITCHURE, S. J. NORTON, Y. GRINBERG and F. BENDEC, *J. Mater. Res.* **8** (1993) 1558.
6. E. P. PAPADAKIS, L. C. LYNNWORTH, K. A. FOWLER and E. H. CARNEVAN, *J. Acoust. Soc. Amer.* **52** (1972) 850.
7. E. P. PAPADAKIS, *J. Test. Eval.* **12** (1984) 273.
8. L. F. BRESSE, D. A. HUTCHINS and K. LUNDGREN, *J. Acoust. Soc. Amer.* **84** (1988) 1751.
9. R. J. DEWHURST, C. EDWARDS, A. D. W. MCKIE and S. B. PALMER, *J. Appl. Phys.* **63** (1988) 1225.
10. R. J. DEWHURST, C. EDWARDS, A. D. W. MCKIE and S. B. PALMER, *Rev. Progr. Quantitative Nondestr. Eval. B* **7** (1988) 1615.
11. J.-D. AUSSEL and J.-P. MONCHALIN, *Ultrasonics* **27** (1989) 165.
12. D. S. FORSYTH, R. D. LEBLANC, A. FAHR, A. MASLOUHI and A. MOREAU, *e-J. Nondestr. Test. Ultrasonics* **2** (1997) (www.ndt.net).
13. C. B. SCRUBY and L. E. DRAIN, "Laser ultrasonics techniques and applications" (Adam Hilger, Bristol, 1990).
14. J.-D. AUSSEL and J.-P. MONCHALIN, *J. Appl. Phys.* **65** (1989) 2922.
15. A. B. BHATIA, *J. Acoust. Soc. Amer.* **31** (1959) 16.
16. L. R. F. ROSE, *ibid.* **75** (1984) 723.
17. P. A. DOYLE, *J. Phys. D* **19** (1986) 1613.
18. K. L. TELSHOW and R. J. CONANT, *J. Acoust. Soc. Amer.* **88** (1990) 1494.
19. J. B. SPICER and J. W. WAGNER, in "Acousto-optics and acoustic microscopy", ASME AMD, Vol. 140, edited by S. M. Gracewski and T. Kundu (American Society of Mechanical Engineers, New York, 1992) p. 163.
20. U. SCHLEICHERT, K. LANGENBERG, W. ARNOLD and S. FAßBENDER, *Rev. Progr. Nondestr. Eval. A* **8** (1989) pp. 489–496.
21. F. A. McDONALD, *Appl. Phys. Lett.* **56** (1990) 230.
22. C. R. BROOKS, "Heat treatment, structure and properties of nonferrous alloys" (American Society for Metals, Metals Park, OH, 1982).
23. J.-P. MONCHALIN, *IEEE Trans. UFFC*, **33** (1986) 485.
24. J. W. WAGNER, in "Physical acoustics", Vol. XIX, edited by W. P. Mason and R. N. Thurston (Academic Press, New York, 1990) p. 201.
25. B. S. BOKSHTEIN, S. Z. BOKSHTEIN and A. A. ZHUKHOVITSKII, "Thermodynamics and Kinetics of Diffusion in Solids" (Oxonian Press, New Delhi, 1985).

Received 9 June 1997
and accepted 11 May 1998